



Minerva Access is the Institutional Repository of The University of Melbourne

Author/s:

Marshall, B;Puthalakath, H;Caria, S;Chugh, S;Doerflinger, M;Colman, PM;Kvansakul, M

Title:

Variola virus F1L is a Bcl-2-like protein that unlike its vaccinia virus counterpart inhibits apoptosis independent of Bim

Date:

2015-01-01

Citation:

Marshall, B., Puthalakath, H., Caria, S., Chugh, S., Doerflinger, M., Colman, P. M. & Kvansakul, M. (2015). Variola virus F1L is a Bcl-2-like protein that unlike its vaccinia virus counterpart inhibits apoptosis independent of Bim. *Cell Death and Disease*, 6 (3), pp.e1680-. <https://doi.org/10.1038/cddis.2015.52>.

Persistent Link:

<https://hdl.handle.net/11343/261408>

License:

[CC BY](#)

Variola virus F1L is a Bcl-2-like protein that unlike its vaccinia virus counterpart inhibits apoptosis independent of Bim

B Marshall^{1,2}, H Puthalakath^{1,2}, S Caria^{1,2}, S Chugh^{1,2,5}, M Doerflinger^{1,2}, PM Colman^{3,4} and M Kvsanakul^{*,1,2,3}

Subversion of host cell apoptosis is an important survival strategy for viruses to ensure their own proliferation and survival. Certain viruses express proteins homologous in sequence, structure and function to mammalian pro-survival B-cell lymphoma 2 (Bcl-2) proteins, which prevent rapid clearance of infected host cells. In vaccinia virus (VV), the virulence factor F1L was shown to be a potent inhibitor of apoptosis that functions primarily by engaging pro-apoptotic Bim. Variola virus (VAR), the causative agent of smallpox, harbors a homolog of F1L of unknown function. We show that VAR F1L is a potent inhibitor of apoptosis, and unlike all other characterized anti-apoptotic Bcl-2 family members lacks affinity for the Bim Bcl-2 homology 3 (BH3) domain. Instead, VAR F1L engages Bid BH3 as well as Bak and Bax BH3 domains. Unlike its VV homolog, variola F1L only protects against Bax-mediated apoptosis in cellular assays. Crystal structures of variola F1L bound to Bid and Bak BH3 domains reveal that variola F1L forms a domain-swapped Bcl-2 fold, which accommodates Bid and Bak BH3 in the canonical Bcl-2-binding groove, in a manner similar to VV F1L. Despite the observed conservation of structure and sequence, variola F1L inhibits apoptosis using a startlingly different mechanism compared with its VV counterpart. Our results suggest that unlike during VV infection, Bim neutralization may not be required during VAR infection. As molecular determinants for the human-specific tropism of VAR remain essentially unknown, identification of a different mechanism of action and utilization of host factors used by a VAR virulence factor compared with its VV homolog suggest that studying VAR directly may be essential to understand its unique tropism.

Cell Death and Disease (2015) 6, e1680; doi:10.1038/cddis.2015.52; published online 12 March 2015

Variola virus (VAR), the causative agent of smallpox, is a member of the poxvirus family and belongs to the orthopoxviridae. Despite its successful eradication nearly 30 years ago, VAR remains an ongoing concern because of its potential use as a bioterrorism agent.¹ The threat of intentional use of VAR coupled with the absence of an FDA-approved drug for the prevention or treatment of smallpox infection is cause for considerable interest in the development of small-molecule therapeutics against VAR. Current strategies for dealing with smallpox are based on vaccination using live vaccinia virus (VV),^{2,3} a closely related member of the orthopoxvirus genus, which shares > 90% sequence identity with VAR. Vaccination using live VV, however, can cause serious complications,⁴ underscoring the need for effective anti-viral treatments, particularly since anti-viral treatment may be a more efficacious strategy compared with vaccination.⁵ Recent strategies to target VAR for small-molecule therapeutics included the use of polymerase inhibitors,⁶ notably Cidofovir, inhibitors of extracellular virus formation⁷ and tyrosine kinase inhibitors including Gleevec.^{8,9} Cidofovir is currently the only approved antiviral drug for the treatment of orthopoxviruses, although it is not approved for smallpox treatment. Other host–virus

interactions have been identified that may be suitable drug targets^{10,11} but currently require further investigation.

Several poxvirus members other than VAR have been shown to rely on virulence factors that prevent premature host cell demise via programmed cell death or apoptosis,^{12–16} thus ensuring survival and proliferation. The B-cell lymphoma 2 (Bcl-2) protein family is a key mediator for maintaining cell survival or to drive apoptosis, thereby removing infected, damaged or unwanted cells,¹⁷ and sequence, structural and functional orthologs of Bcl-2 have been found in a number of poxviruses.¹⁸ Certain viral Bcl-2-like proteins were only identified as family members after their 3D structures were determined, owing to their complete lack of sequence identity to mammalian Bcl-2 proteins. This group of proteins include the myxoma virus M11L¹² and VV F1L¹⁵ and N1L.¹⁹ Myxoma virus M11L was shown to adopt the classical Bcl-2 fold^{20,21} that utilizes the canonical Bcl-2 homology 3 (BH3)-binding groove to engage BH3 ligands to exert its pro-survival effect. VV F1L also adopts a Bcl-2 fold, but unlike M11L it exists as a domain-swapped dimer,^{22,23} whereas N1L also adopted a dimeric Bcl-2 fold but with a different dimeric arrangement.^{24,25}

Although F1L from VAR has not previously been investigated, the VV homolog is well characterized. VV F1L has been

¹Department of Biochemistry, La Trobe University, Kingsbury Drive, Melbourne, 3086 Victoria, Australia; ²La Trobe Institute for Molecular Science, La Trobe University, Kingsbury Drive, Melbourne, 3086 Victoria, Australia; ³Walter and Eliza Hall Institute of Medical Research, 1G Royal Parade, Parkville, 3052 Victoria, Australia and ⁴Department of Medical Biology, University of Melbourne, Parkville, Victoria 3010, Australia

*Corresponding author: M Kvsanakul, Department of Biochemistry, La Trobe University, Kingsbury Drive, Bundoora, 3086 Victoria, Australia. Tel: +61 3 9479 2263; Fax: +61 3 9479 2467. E-mail: m.kvsanakul@latrobe.edu.au

⁵Current address: CSL Limited, Bio21 Institute, 30 Flemington Road, Parkville, Victoria 3052, Australia

Abbreviations: Bcl-2, B-cell lymphoma 2; VAR, variola virus; VV, vaccinia virus; BH, Bcl-2 homology; MEF, mouse embryonic fibroblast

Received 26.7.14; revised 26.1.15; accepted 27.1.15; Edited by R Johnston

shown to inhibit the mitochondrial pathway of apoptosis by replacing Mcl-1²⁶ and interacts with the isolated BH3 domains of Bim, Bax and Bak,²³ which are bound in the canonical Bcl-2-binding groove.²² Furthermore, an F1L-deficient VV potently causes Bak/Bax-mediated apoptosis.^{15,27} Functionally, VV F1L appears to rely primarily on neutralization of Bim in the context of a viral infection.²² Given the close similarity between VAR and VV, VAR may also rely on inhibition of host cell apoptosis for successful infection and proliferation. Disruption of VAR ability to inhibit apoptosis thus may constitute an attractive strategy for small-molecule-based intervention. To investigate this possibility, we performed a biochemical, structural and functional characterization of VAR F1L. Here we report that despite possessing a nearly identical 3D structure and sequence, VAR F1L inhibits apoptosis via a different mechanism compared with its homolog in VV.

Results

Given the high sequence identity of VAR F1L with VV F1L (Figure 1a) and the location of primary sequence variations (all of which are away from the identified BH3-domain-binding groove in VV F1L (Figure 1b and Supplementary Figure 1)), we surmised that VAR F1L would display a ligand-binding behavior similar to VV F1L. Using recombinant VAR F1L we tested a panel of pro-apoptotic BH3-domain ligands using isothermal calorimetry (Figure 1c). Previously, we showed that VV F1L exhibited a highly selective BH3-domain ligand-binding profile, with high affinity for pro-apoptotic Bim ($K_D = 200$ nM), and considerably lower affinity for Bax and Bak BH3 domains (K_D of 2000 and 4300 nM, respectively).²³ Similarly, VAR F1L bound Bax and Bak BH3 domains weakly with K_D values of 920 and 2640 nM, respectively. Unexpectedly, VAR F1L showed no detectable affinity for Bim BH3, and only weakly bound Bid from the BH3-only proteins with a K_D of 3220 nM. Considering the weak affinity of VAR F1L for Bax and Bak BH3 ligands, we then investigated if VAR F1L is able to engage and restrain full-length Bax and Bak. For this purpose, we utilized a yeast-based assay in which we expressed full-length Bak, Bax and VAR F1L. The assay is based on the observation that Bax or Bak overexpression is lethal in yeast, but can be repressed by co-expression of Bcl-2, Bcl-x_L, Mcl-1 or A1. Similar to endogenous mammalian

pro-survival Bcl-2, VAR F1L is able to prevent both Bak- and Bax-induced yeast death (Supplementary Figure 2), indicating that VAR F1L is able to directly engage both Bak and Bax. In contrast, VV F1L has only been shown to bind Bak but not Bax in yeast (Supplementary Figure 2), as previously observed in mammalian cells.²⁸

Structural basis for VAR F1L BH3 domain ligand binding.

To investigate the molecular basis for Bid, Bak and Bax BH3 domain binding by VAR F1L, we determined crystal structures of VAR F1L in complex with Bak and Bid BH3 domain peptides (Figures 2a and d, Table 1). As observed previously for VV F1L,^{22,23} VAR F1L adopts a Bcl-2-like fold that forms a domain-swapped Bcl-2 with similar binding grooves that engage BH3-domain ligands (Figures 2b and e). Superimposition of bound Bak and Bid BH3 backbones indicate that both ligands are bound in near identical manner (Supplementary Figures 3a and b). In the VAR F1L:Bak BH3 complex (Figure 2c), residues V75, L78, I81, I85 protrude into four pockets in the VAR F1L-binding groove, similar to the equivalent hydrophobic residues in Bid (Figure 2f; I86, L90, V93, M97).

Comparison of VAR_F1L:Bak BH3 with VV_F1L:Bak BH3 complex.

Superimposition of VV F1L with VAR F1L from their respective complexes with Bak BH3 yields a root-mean-square deviation of 0.9 Å over 138 Ca atoms, with the only notable differences in side chain orientations between VV F1L and VAR F1L occurring at F135 (Supplementary Figure 4). Overall, the VV F1L and VAR_F1L complexes with Bak appear to be near identical.

VAR F1L only inhibits Bax but not Bak-mediated apoptosis.

To identify differences in anti-apoptotic activity between VAR and VV F1L, we retrovirally transfected VAR F1L into wild-type, Bax^{-/-}, Bak^{-/-} and Bax^{-/-}/Bak^{-/-} DKO cells and treated them with thapsigargin to induced apoptosis via ER stress. Unexpectedly, VAR F1L was unable to protect both wild-type and Bax^{-/-} mouse embryonic fibroblasts (MEFs), whereas Bak^{-/-} MEFs were efficiently protected from apoptosis (Figure 3a) in a manner similar to Bcl-2 (Figure 3b), suggesting that VAR F1L exclusively inhibits Bax-mediated apoptosis. Similar results were obtained after serum

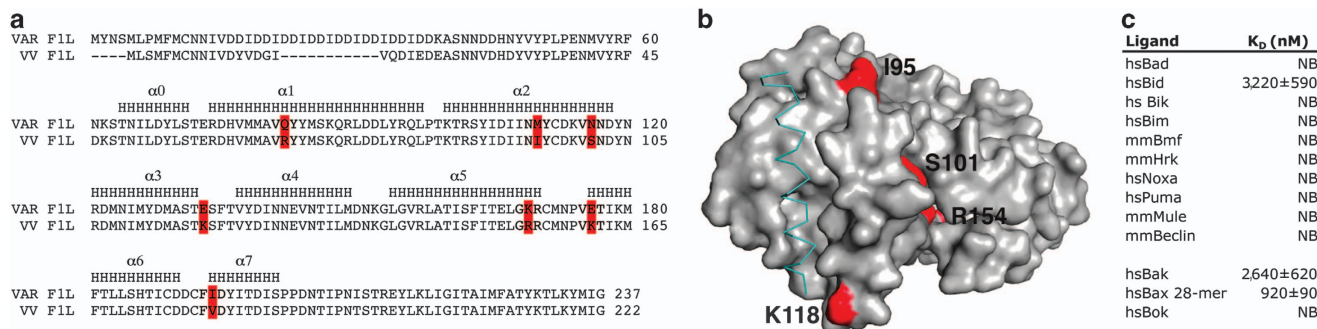


Figure 1 (a) Sequence alignment of vaccinia virus (VV) with variola virus (VAR) F1L. Red denotes sequence differences in the Bcl-2 domain, H indicates helices. (b) Sequence variations between VV and VAR F1L are mapped in red on a molecular surface of VV F1L (gray). (c) BH3-binding profile of VAR_F1L. K_D values were determined by isothermal calorimetry

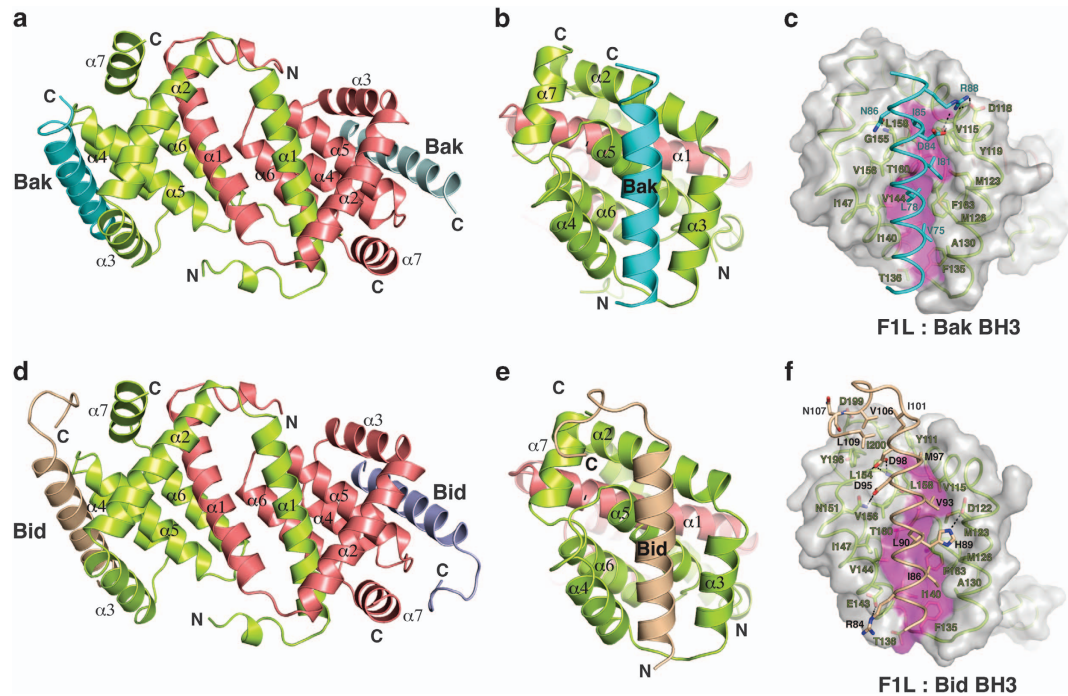


Figure 2 Structures of VAR F1L:Bak and Bid BH3 complexes. **(a)** Cartoon diagram of F1L:Bak BH3 complex. F1L chains are shown as a cartoon (lime and salmon), with helices α 1-7 labeled. Two Bak BH3 chains are shown in cyan and light blue. **(b)** Cartoon diagram of F1L:Bak BH3 complex. This view looks into the hydrophobic BH3-binding groove, which is formed by helices α 2-5. F1L helices α 2-7 from monomer 1 (lime) are labeled, as is helix α 1' from monomer 2 (salmon). Bak BH3 is shown in cyan. **(c)** Cartoon diagram of F1L:Bid BH3 complex. F1L (lime and salmon) in complex with Bid BH3 (wheat and lilac). The view is as in **a**. **(d)** Cartoon diagram of F1L:Bid BH3 complex. This view is as in **b**. F1L helices α 2-7 from monomer 1 (lime) are labeled, as is helix α 1' from monomer 2 (salmon). Bid BH3 is shown in wheat. **(e)** Stereo diagram of the F1L (lime):Bak (cyan) complex interface. The F1L surface is shown in gray, except for magenta shading indicating the floor of the peptide-binding groove. F1L residues are labeled in lime, Bim BH3 residues are labeled in cyan. **(f)** Stereo diagram of the F1L (lime):Bid (wheat) complex interface. View and labeling is as in **c**, except for labeling of Bid residues (in black)

Table 1 Crystallographic statistics

Crystal	F1L: Bak	F1L: Bid
<i>Data collection and phasing</i>		
Spacegroup	I2	F222
Resolution range (Å)	40 - 2.55	50 - 1.75
Unique reflections	45043	17113
Multiplicity ^a	4.1 (4.1)	13.3 (9.2)
Completeness (%) ^a	99.9 (100.0)	97.1 (80.4)
$R_{\text{merge}}^{\text{a,b}}$	0.075 (0.656)	0.062 (0.459)
Mn $I/\sigma I$	12.0 (2.2)	39.0 (4.1)
<i>Refinement</i>		
Resolution range (Å)	39.7 - 2.55	40.5 - 1.75
Reflections (working set/test set)	41807/2127	15817/842
Protein atoms	7943	1351
Solvent atoms	98 H ₂ O	91 H ₂ O
$R_{\text{cryst}}/R_{\text{free}}^{\text{c}}$	0.197/0.242	0.172/0.213
r.m.s.d. bonds (Å)	0.002	0.012
r.m.s.d. angles (°)	0.5	1.2
Ramachandran plot (%) ^d	95.1/4.9/0.0/0.0	98.0/2.0/0.0/0.0

^aNumbers in parentheses refer to the highest resolution shells. ^b $R_{\text{merge}} = \sum_p \sum_i |I_i(h) - \langle I(h) \rangle| / \sum_p \sum_i I_i(h)$, where $I_i(h)$ is the i th measurement of reflection h and $\langle I(h) \rangle$ is the weighted mean of all measurements of h . ^c $R = \sum_p |F_{\text{obs}} - F_{\text{calc}}| / \sum_p F_{\text{obs}}$, where F_{obs} and F_{calc} are the observed and calculated structure factor amplitudes, respectively. R_{cryst} and R_{free} were calculated using the working and test set, respectively. ^dResidues in most favoured, additionally allowed, generously allowed and disallowed regions

withdrawal, with VAR F1L maintaining viability of Bak^{-/-} MEFs but not wild-type and Bax^{-/-} MEFs (Supplementary Figure 5). Overall, the cellular assays mirror our peptide-binding data obtained by ITC, where the lower affinity ligand Bak is not

inhibited in a cellular context. Considering the peptide-binding data, we next investigated whether VAR F1L is able to protect against Bim- and Bid-induced apoptosis. 293T cells were transfected with either Bim_{EL} or Bid. VAR F1L protected against both Bim_{EL} ($P=0.006$) or Bid-mediated apoptosis ($P=0.0027$), with comparable levels of protection observed with Bcl-2.

Discussion

Interactions between pro- and anti-apoptotic Bcl-2 family members are critical for the regulation of apoptosis during normal development as well as during disease states including viral infections or cancer.¹⁷ Compelling evidence points to a critical role for viral Bcl-2 proteins during the viral life cycle, particularly viral infectivity and proliferation.^{12,15,29} No anti-apoptotic activity for VAR encoded proteins has been demonstrated to date, although a number of proteins from the closely related VV have been reported to manipulate host cell death signaling.^{15,30} We have now shown biochemically that VAR F1L is able to engage a limited number of pro-apoptotic Bcl-2 proteins including Bid, Bak and Bax. This binding profile is highly unusual, as all reported cellular or viral anti-apoptotic Bcl-2 family members engage Bim,³¹ the sole pan pro-survival antagonist of the Bcl-2 family,³² making VAR F1L the first reported exception. This observation was unexpected as VV F1L binds Bim BH3 *in vitro* and *in vivo*.^{22,28} Furthermore, VV F1L prevents both Bak- and Bax-mediated apoptosis in cell-based assays,^{26,28} whereas

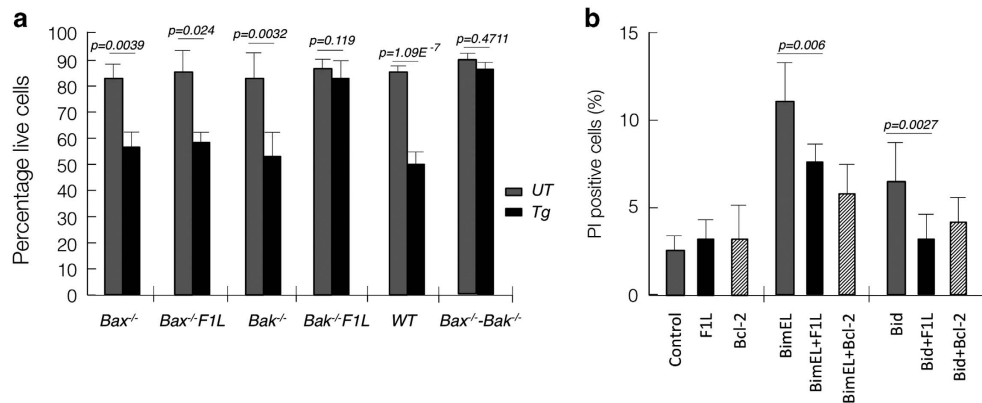


Figure 3 VAR F1L inhibits Bax- but not Bak-mediated apoptosis. (a) Viability of wild-type, *Bax*^{-/-}, *Bak*^{-/-} and *Bax*^{-/-}/*Bak*^{-/-} DKO cells. MEF cells stably overexpressing VAR F1L or vector, treated with 1.5 μ M thapsigargin and cultured for 24 h. (b) Viability of 293T cells transiently overexpressing either Bim_{EL} or Bid as well as F1L, Bcl-2 or vector control. Error bars are \pm S.E.M. with $n=3$

VAR F1L was able to neutralize only Bax-mediated apoptosis. Close examination of structures of VAR F1L complexes with Bid and Bak and VV F1L complexes with Bim and Bak did not reveal major differences in BH3 domain binding to the canonical binding groove (Supplementary Figure 4) that can explain the startlingly different ligand-binding behavior. The loss of Bim binding for VAR F1L is particularly noteworthy as VV-induced apoptosis is reduced in Bim-deficient cells,²⁸ suggesting that Bim plays a substantial role during the cellular response to VV infection. Whether or not Bim is important for VAR infection has not been determined to date. In the case of Epstein-Barr virus BHRF1-mediated inhibition of apoptosis, Bim³³ and Bak³⁴ neutralization were shown to be critical, whereas in the case of myxoma virus M11L,²⁰ Bax and Bak sequestration were identified as the primary mechanism of inhibition. However, in both cases, the mechanism of apoptosis inhibition was not defined in the context of a viral infection. Nonetheless, despite the inability to directly engage Bim, and the very modest affinity to Bid, VAR F1L is able to counter both Bim- and Bid-mediated apoptosis.

In addition to raising intriguing questions about VAR biology, this striking insensitivity of VAR F1L to Bim raises questions about the regulation of Bcl-2-mediated apoptosis. Direct activation of Bax and Bak via promiscuous or activator BH3-only proteins has been shown to be an important route to trigger apoptosis,³⁵⁻³⁸ however, VAR F1L appears to be unlikely to act by BH3-only protein sequestration to prevent Bax activation. Among the other alternatively proposed mechanisms invoked to control apoptosis, VAR F1L's ability to inhibit apoptosis is most readily explained by an indirect model based on sequestration of Bax and Bak,^{39,40} where Bax and Bak are held in an inactive configuration by a pro-survival Bcl-2 family member. This is supported by our observations that VAR F1L is able to bind BH3 domain peptides from Bax and Bak, albeit at modest affinity, as well as the prevention of Bax- and Bak-induced growth arrest in yeast-based assays in the absence of any other cellular apoptosis regulatory proteins. Such a mechanism is also an integral part of the currently favored unified model,⁴¹ where a balance between direct activation and indirect activation ultimately yields control of intrinsic apoptosis. The insensitivity of VAR F1L to Bim, and indeed all tested BH3-only proteins, is striking in this context,

and may make VAR F1L a useful tool molecule to further understand the interplay of the two main modes that underpin the unified model of apoptosis regulation.

Targeting of the apoptotic machinery is currently an intensely pursued strategy for the development of novel drugs for cancer therapy.^{42,43} Similarly, VAR F1L may be a valid target for development of antiviral therapeutics. Current strategies for the development of antiviral therapeutics against VAR have relied mostly on the use of homologous target molecules from VV, monkeypox or ectromelia virus, with only a small number of studies utilizing VAR-encoded proteins,⁴⁴⁻⁴⁶ and even fewer studies using their structures.^{47,48} The marked differences between VAR and VV F1L suggest that studies of VAR proteins may provide unexpected avenues for therapeutic intervention that may not be predicted based on available data from the closely related and much better understood VV. It also raises the question of how well current systems that mimic VAR model the behavior of this intriguing virus. VAR occupies a unique position as the sole human pathogen among the orthopoxviruses. As molecular determinants for this human-specific tropism remain essentially unknown, identification of a different mechanism of action and utilization of host factors used by a VAR virulence factor compared with its VV homolog suggest that studying VAR directly may be essential to understand its unique tropism.

Materials and Methods

All experiments were performed with WHO approval

Recombinant proteins and binding experiments: VAR_F1L Δ N38 Δ C36 was amplified by PCR from expression-optimized F1L cDNA (Blue Heron), cloned into the pGEX-6P3 vector (Invitrogen, Melbourne, VIC, Australia) using *Bam*HI and *Eco*RI, and expressed in *E. coli* BL21 DE3 pLysS cells. Cells were homogenized using an Avestin EmulsiFlex homogenizer in lysis buffer (50 mM Tris-HCl, pH 8.0, 150 mM NaCl, 1 mM EDTA). After centrifugation, the supernatant was applied to a glutathione sepharose column (GE Healthcare, Melbourne, VIC, Australia) and washed with lysis buffer. On-column cleavage was performed using Prescission Protease (GE Healthcare), and VAR F1L was eluted using lysis buffer. Subsequently, VAR F1L was subjected to gel-filtration chromatography in 25 mM HEPES, pH 7.5, 150 mM NaCl using a Superdex 200 column (GE Healthcare). Calorimetry data were collected on a VP-ITC (MicroCal) with VAR_F1L Δ N38 Δ C36 as previously described.²³ Peptides used have been described previously.³⁴

Crystallization and structure determination: VAR F1L:Bak or VAR F1L:Bid BH3 complexes were obtained by mixing VAR F1L with human Bak 26-mer or Bid

34-mer peptide in a 1:1.25 molar ratio and concentrated using a centricon (Millipore) to 5 mg/ml.

VAR F1L:Bak BH3 crystals were grown by the sitting drop method at room temperature in 1.7 M MgSO₄, 0.1 M sodium acetate with pH 5.2. The crystals belong to space group I121 with $a = 124.774 \text{ \AA}$, $b = 68.762 \text{ \AA}$, $c = 171.598 \text{ \AA}$, $\alpha = 90^\circ$, $\beta = 109.43^\circ$, $\gamma = 90^\circ$. The asymmetric unit contains six VAR F1L chains and six Bak BH3 peptides, with 49% solvent content. Diffraction data were collected from crystals flash frozen in paratone at 100 K using beamline MX2 at the Australian Synchrotron (Melbourne, VIC, Australia).

VAR F1L:Bid BH3 crystals were grown by the sitting drop method at room temperature in 1.8 M sodium acetate and 0.1 M HEPES (pH 6.5). The crystals belong to space group I121 with $a = 124.774 \text{ \AA}$, $b = 68.762 \text{ \AA}$, $c = 171.598 \text{ \AA}$, $\alpha = 90^\circ$, $\beta = 109.43^\circ$, $\gamma = 90^\circ$. The asymmetric unit contains one VAR F1L chain and one Bid BH3 peptides, with 49% solvent content. Diffraction data were collected from crystals flash frozen in paratone at 100 K using beamline MX2 at the Australian Synchrotron.

Diffraction data were processed with XDS⁴⁹ and programs of the CCP4 suite.⁵⁰ The VAR F1L:Bak BH3 and VAR F1L:Bid BH3 structures were solved by molecular replacement with PHASER⁵¹ using F1L from the VV F1L structure as a search model (PDB 2VTY) and refined using Phenix.⁵² All data collection and refinement statistics are summarized in Supplementary Table 1. Figures were prepared using PyMol.⁵³ Software was in some instances accessed via SGrid.⁵⁴

Yeast colony assays

Saccharomyces cerevisiae. W303 α cells were co-transformed with pGALL(TRP) vector only, pGALL(TRP)-Bcl-x_L, or pGALL(TRP)-VAR_F1L and pGALL(Leu)-Bak or pGALL(Leu)-Bax. pGALL(TRP) and pGALL(Leu) places genes under the control of a galactose inducible promoter. Cells were spotted as fivefold serial dilutions onto medium containing 2% (w/v) galactose (inducing, 'ON'), which induces protein expression, or 2% (w/v) glucose (repressing, 'OFF'), which prevents protein expression, as previously described.⁵⁵ Plates were incubated for 48 h at 30 °C and then photographed.

Cell culture, transfection, lentiviral infection and cellular assays: Human embryonic kidney 293T (ATCC CRL-3216) and MEFs (a gift from D Huang) were cultured in Dubecco's modified Eagle's medium supplemented with 10% fetal calf serum (Sigma) at 37 °C in a humidified 10% CO₂ incubator. Both *bak*^{-/-} and *bax*^{-/-} MEFs were generated from E15 embryos in accordance with standard procedures and were infected with SV40 large T antigen-expressing lentiviruses as described.^{39,40}

To generate lentiviral particles, human embryonic kidney 293T cells were transfected with packaging constructs pCMV δ R8.2 and VSVg and the relevant lentiviral plasmid at a ratio of 1:0.4:0.6 using Fugene 6.0 transfection reagent (Roche Lifesciences, Indianapolis, IN, USA) following the manufacturer's instructions. The virus containing supernatants were harvested, filtered (0.8 μ m) and supplemented with polybrene (4 mg/ml). Target cells were infected with virus supernatant as described by Vince et al.⁵⁶

MEF cells were seeded at ~10 000 cells per well and allowed to adhere for 24 h. The cells were then treated with Thapsigargin (1.5 μ M final, Calbiochem, San Diego, CA, USA) or serum withdrawal for 24 and 48 h. To monitor cell death, cells were stained with propidium iodide (1.25 μ g/ml) and analyzed in a FACScan (Becton Dickinson). Values presented are the means \pm S.D. ($n = 3$). Differences were considered significant at $P < 0.05$.

293T cells were seeded @150 000 cells per well in six-well plates in complete Dubecco's modified Eagle's medium and incubated O/N @37 °C, 5% CO₂. Next day, the cells were transfected with 0.25 μ g Bim, Bid or Bcl2 and 0.5 μ g F1L or control plasmid DNA per well using Xtreme Gene 9 transfection reagent (Roche Lifesciences; Catalog number 06365787001). 24 h post transfection, cells were harvested by trypsinization and PI uptake measured by flow cytometry. Error bars presented are the standard error of the means ($n = 3$).

Conflict of Interest

The authors declare no conflict of interest.

Acknowledgements. We thank A Wardak for technical assistance; staff at the Australian Synchrotron for assistance with diffraction data collection; CSIRO C3 Centre for assistance with crystallization. This work was supported by the National Health and Medical Research Council Australia (Project Grant APP1007918 and

Fellowship 637372 to MK, Fellowship and Program Grant to PMC), Australian Research Council (Fellowship FT130101349 to MK), the Cooperative Research Center for Biomarker Translation (scholarship to BM), the Victorian State Government Operational Infrastructure Support and the Australian Government NHMRC IIRISS. **Data deposition:** Coordinates for F1L were deposited with the Protein Data Bank, accession code 5ajj and 5ajk.

- Kaiser J. Smallpox vaccine. A tame virus runs amok. *Science* 2007; **316**: 1418–1419.
- Poland GA, Grabenstein JD, Neff JM. The US smallpox vaccination program: a review of a large modern era smallpox vaccination implementation program. *Vaccine* 2005; **23**: 2078–2081.
- Jacobs BL, Langland JO, Kibler KV, Denzler KL, White SD, Holecck SA et al. Vaccinia virus vaccines: past, present and future. *Antiviral Res* 2009; **84**: 1–13.
- Bray M. Pathogenesis and potential antiviral therapy of complications of smallpox vaccination. *Antiviral Res* 2003; **58**: 101–114.
- Stittelaar KJ, Neyts J, Naesens L, van Amerongen G, van Lavieren RF, Holy A et al. Antiviral treatment is more effective than smallpox vaccination upon lethal monkeypox virus infection. *Nature* 2006; **439**: 745–748.
- Baker R, Bray M, Huggins JW. Potential antiviral therapeutics for smallpox, monkeypox and other orthopoxvirus infections. *Antiviral Res* 2003; **57**: 13–23.
- Yang G, Pevear DC, Davies MH, Collett MS, Bailey T, Rippen S et al. An orally bioavailable antipoxvirus compound (ST-246) inhibits extracellular virus formation and protects mice from lethal orthopoxvirus challenge. *J Virol* 2005; **79**: 13139–13149.
- Reeves PM, Bommaribus B, Lebeis S, McNulty S, Christensen J, Swimm A et al. Disabling poxvirus pathogenesis by inhibition of Abl-family tyrosine kinases. *Nat Med* 2005; **11**: 731–739.
- Yang HL, Kim SK, Kim M, Reche PA, Morehead TJ, Damon IK et al. Antiviral chemotherapy facilitates control of poxvirus infections through inhibition of cellular signal transduction. *J Clin Invest* 2005; **115**: 379–387.
- Fauci AS, Challberg MD. Host-based antipoxvirus therapeutic strategies: turning the tables. *J Clin Invest* 2005; **115**: 231–233.
- Sliva K, Schnierle B. From actually toxic to highly specific - novel drugs against poxviruses. *Viral J* 2007; **4**: 8.
- Graham KA, Oppenorth A, Upton C, McFadden G. Myxoma virus M11L ORF encodes a protein for which cell surface localization is critical in manifestation of viral virulence. *Virology* 1992; **191**: 112–124.
- Banadaya L, Lam SC, Okamoto T, Kvensakul M, Huang DC, Barry M. Deerpox virus encodes an inhibitor of apoptosis that regulates Bak and Bax. *J Virol* 2011; **85**: 1922–1934.
- Banadaya L, Veugelers K, Campbell S, Barry M. The fowlpox virus BCL-2 homologue, FPV039, interacts with activated Bax and a discrete subset of BH3-only proteins to inhibit apoptosis. *J Virol* 2009; **83**: 7085–7098.
- Wasilenko ST, Stewart TL, Meyers AF, Barry M. Vaccinia virus encodes a previously uncharacterized mitochondrial-associated inhibitor of apoptosis. *Proc Natl Acad Sci USA* 2003; **100**: 14345–14350.
- Okamoto T, Campbell S, Mehta N, Thibault J, Colman PM, Barry M et al. Sheeppox virus SPPV14 encodes a Bcl-2-like cell death inhibitor that counters a distinct set of mammalian proapoptotic proteins. *J Virol* 2012; **86**: 11501–11511.
- Youle RJ, Strasser A. The BCL-2 protein family: opposing activities that mediate cell death. *Nat Rev Mol Cell Biol* 2008; **9**: 47–59.
- Kvensakul M, Hinds MG. Structural biology of the Bcl-2 family and its mimicry by viral proteins. *Cell Death Dis* 2013; **4**: e909.
- Bartlett N, Symons JA, Tschärke DC, Smith GL. The vaccinia virus N1L protein is an intracellular homodimer that promotes virulence. *J Gen Virol* 2002; **83**: 1965–1976.
- Kvensakul M, van Delft MF, Lee EF, Gulbis JM, Fairlie WD, Huang DC et al. A structural viral mimic of pro-survival bcl-2: a pivotal role for sequestering proapoptotic bax and bak. *Mol Cell* 2007; **25**: 933–942.
- Douglas AE, Corbett KD, Berger JM, McFadden G, Handel TM. Structure of M11L: A myxoma virus structural homolog of the apoptosis inhibitor, Bcl-2. *Protein Sci* 2007; **16**: 695–703.
- Campbell S, Thibault J, Mehta N, Colman PM, Barry M, Kvensakul M. Structural insight into BH3 domain binding of vaccinia virus antiapoptotic F1L. *J Virol* 2014; **88**: 8667–8677.
- Kvensakul M, Yang H, Fairlie WD, Czabotar PE, Fischer SF, Perugini MA et al. Vaccinia virus anti-apoptotic F1L is a novel Bcl-2-like domain-swapped dimer that binds a highly selective subset of BH3-containing death ligands. *Cell Death Differ* 2008; **15**: 1564–1571.
- Aoyagi M, Zhai D, Jin C, Aleshin AE, Stec B, Reed JC et al. Vaccinia virus N1L protein resembles a B cell lymphoma-2 (Bcl-2) family protein. *Protein Sci* 2007; **16**: 118–124.
- Cooray S, Bahar MW, Abrescia NG, McVey CE, Bartlett NW, Chen RA et al. Functional and structural studies of the vaccinia virus virulence factor N1 reveal a Bcl-2-like anti-apoptotic protein. *J Gen Virol* 2007; **88**: 1656–1666.
- Campbell S, Hazes B, Kvensakul M, Colman P, Barry M. Vaccinia virus F1L interacts with Bak using highly divergent Bcl-2 homology domains and replaces the function of Mcl-1. *J Biol Chem* 2010; **285**: 4695–4708.
- Fischer SF, Ludwig H, Holzappel J, Kvensakul M, Chen L, Huang DCS et al. Modified vaccinia virus ankara protein F1L is a novel BH3-domain binding protein and acts together

- with the early viral protein E3L to block virus-associated apoptosis. *Cell Death Differ* 2006; **13**: 109–118.
28. Taylor JM, Quilty D, Banadyga L, Barry M. The vaccinia virus protein F1L interacts with Bim and inhibits activation of the pro-apoptotic protein Bax. *J Biol Chem* 2006; **281**: 39728–39739.
 29. Altmann M, Hammerschmidt W. Epstein-Barr virus provides a new paradigm: a requirement for the immediate inhibition of apoptosis. *PLoS Biol* 2005; **3**: e404.
 30. Dobbstein M, Shenk T. Protection against apoptosis by the vaccinia virus SPI-2 (B13R) gene product. *J Virol* 1996; **70**: 6479–6485.
 31. Kvensakul M, Hinds MG. The structural biology of BH3-only proteins. *Meth Enzym* 2014; **544**: 49–74.
 32. Rautureau GJ, Yabal M, Yang H, Huang DC, Kvensakul M, Hinds MG. The restricted binding repertoire of Bcl-B leaves Bim as the universal BH3-only pro-survival Bcl-2 protein antagonist. *Cell Death Dis* 2012; **3**: e443.
 33. Desbien AL, Kappler JW, Marrack P. The Epstein-Barr virus Bcl-2 homolog, BHRF1, blocks apoptosis by binding to a limited amount of Bim. *Proc Natl Acad Sci USA* 2009; **106**: 5663–5668.
 34. Kvensakul M, Wei AH, Fletcher JI, Willis SN, Chen L, Roberts AW *et al*. Structural basis for apoptosis inhibition by Epstein-Barr virus BHRF1. *PLoS Pathog* 2010; **6**: e1001236.
 35. Czabotar PE, Westphal D, Dewson G, Ma S, Hockings C, Fairlie WD *et al*. Bax crystal structures reveal how BH3 domains activate bax and nucleate its oligomerization to induce apoptosis. *Cell* 2013; **152**: 519–531.
 36. Du H, Wolf J, Schafer B, Moldoveanu T, Chipuk JE, Kuwana T. BH3 domains other than Bim and Bid can directly activate Bax/Bak. *J Biol Chem* 2011; **286**: 491–501.
 37. Gavathiotis E, Reyna DE, Davis ML, Bird GH, Walensky LD. BH3-triggered structural reorganization drives the activation of proapoptotic BAX. *Mol Cell* 2010; **40**: 481–492.
 38. Chi X, Kale J, Leber B, Andrews DW. Regulating cell death at, on, and in membranes. *Biochim Biophys Acta* 2014; **1843**: 2100–2113.
 39. Willis SN, Chen L, Dewson G, Wei A, Naik E, Fletcher JI *et al*. Pro-apoptotic Bak is sequestered by Mc1-1 and Bcl-xL, but not Bcl-2, until displaced by BH3-only proteins. *Genes Devel* 2005; **19**: 1294–1305.
 40. Willis SN, Fletcher JI, Kaufmann T, van Delft MF, Chen L, Czabotar PE *et al*. Apoptosis initiated when BH3 ligands engage multiple Bcl-2 homologs, not Bax or Bak. *Science* 2007; **315**: 856–859.
 41. Llambi F, Moldoveanu T, Tait SW, Bouchier-Hayes L, Temirov J, McCormick LL *et al*. A unified model of mammalian BCL-2 protein family interactions at the mitochondria. *Mol Cell* 2011; **44**: 517–531.
 42. Lessene G, Czabotar PE, Colman PM. BCL-2 family antagonists for cancer therapy. *Nat Rev Drug Discov* 2008; **7**: 989–1000.
 43. Kvensakul M, Hinds MG. The Bcl-2 family: structures, interactions and targets for drug discovery. *Apoptosis* 2015; **20**: 136–150.
 44. Aleshin AE, Drag M, Gombosuren N, Wei G, Mikolajczyk J, Satterthwait AC *et al*. Activity, specificity, and probe design for the smallpox virus protease K7L. *J Biol Chem* 2012; **287**: 39470–39479.
 45. Gileva IP, Nepomnyashchikh TS, Ryazankin IA, Shchelkunov SN. Recombinant TNF-binding protein from variola virus as a novel potential TNF antagonist. *Biochem Biokhimiia* 2009; **74**: 1356–1362.
 46. Mohamed MR, Rahman MM, Lanchbury JS, Shattuck D, Neff C, Dufford M *et al*. Proteomic screening of variola virus reveals a unique NF-kappaB inhibitor that is highly conserved among pathogenic orthopoxviruses. *Proc Natl Acad Sci USA* 2009; **106**: 9045–9050.
 47. Perry K, Hwang Y, Bushman FD, Van Duyn GD. Structural basis for specificity in the poxvirus topoisomerase. *Mol Cell* 2006; **23**: 343–354.
 48. Phan J, Tropea JE, Waugh DS. Structure-assisted discovery of Variola major H1 phosphatase inhibitors. *Acta Cryst D* 2007; **63**: 698–704.
 49. Kabsch W. Xds. *Acta Cryst D* 2010; **66**: 125–132.
 50. Winn MD, Ballard CC, Cowtan KD, Dodson EJ, Emsley P, Evans PR *et al*. Overview of the CCP4 suite and current developments. *Acta Cryst D* 2011; **67**: 235–242.
 51. Storoni LC, McCoy AJ, Read RJ. Likelihood-enhanced fast rotation functions. *Acta Cryst D* 2004; **60**: 432–438.
 52. Adams PD, Afonine PV, Bunkoczi G, Chen VB, Davis IW, Echols N *et al*. PHENIX: a comprehensive Python-based system for macromolecular structure solution. *Acta Cryst D* 2010; **66**: 213–221.
 53. DeLano WL. The PyMOL molecular graphics system, 2002. www.pymol.org.
 54. Morin A, Eisenbraun B, Key J, Sanschagrin PC, Timony MA, Ottaviano M *et al*. Collaboration gets the most out of software. *eLife* 2013; **2**: e01456.
 55. Jabbour AM, Puryer MA, Yu JY, Lithgow T, Riffkin CD, Ashley DM *et al*. Human Bcl-2 cannot directly inhibit the *Caenorhabditis elegans* Apaf-1 homologue CED-4, but can interact with EGL-1. *J Cell Sci* 2006; **119**: 2572–2582.
 56. Vince JE, Wong W, Khan N, Feltham R, Chau D, Ahmed AU *et al*. IAP antagonists target cIAP1 to induce TNF α -dependent apoptosis. *Cell* 2007; **131**: 682–693.



Cell Death and Disease is an open-access journal published by Nature Publishing Group. This work is licensed under a Creative Commons Attribution 4.0 International License. The images or other third party material in this article are included in the article's Creative Commons license, unless indicated otherwise in the credit line; if the material is not included under the Creative Commons license, users will need to obtain permission from the license holder to reproduce the material. To view a copy of this license, visit <http://creativecommons.org/licenses/by/4.0/>

Supplementary Information accompanies this paper on Cell Death and Disease website (<http://www.nature.com/cddis>)